

Plasmonic Nanoantennas for Broad-Band Enhancement of Two-Photon Emission from Semiconductors

Amir Nevet,* Nikolai Berkovitch, Alex Hayat, Pavel Ginzburg, Shai Ginzach, Ofir Sorias, and Meir Orenstein

Department of Electrical Engineering, Technion, Haifa 32000, Israel

ABSTRACT We demonstrate experimentally and theoretically a broad-band enhancement of the spontaneous two-photon emission from AlGaAs at room temperature by plasmonic nanoantenna arrays fabricated on the semiconductor surface. Plasmonic structures with inherently low quality factors but very small effective volumes are shown to be optimal. A 20-fold enhancement was achieved for the entire antenna array, corresponding to an enhancement of nearly 3 orders of magnitude for charge carriers emitting at the near field of a plasmonic antenna.

KEYWORDS Semiconductors, two-photon emission, nanoparticles, plasmonic enhancement

Over the past decade, a growing interest has been focused on exploiting the tight confinement of the electromagnetic field achievable in the vicinity of a metal–dielectric boundary, commonly referred to as surface plasmon polariton (SPP), for enhancing the efficiency of spontaneous emission in semiconductors,^{1–3} and it has been shown that such enhancement is highly significant for very inefficient emitters.⁴ These endeavors follow the success of using SPPs for the enhancement of nonlinear phenomena, including the surface enhancement of Raman scattering by many orders of magnitude,⁵ surface-enhanced second-harmonic generation,⁶ and the recent demonstration of high-harmonic generation by coupling to bow-tie nanoantennas.⁷ It was also shown that SPPs preserve many key quantum properties of the photons used to excite them, including entanglement,^{8,9} and the quantization theory of surface plasmon fields was developed¹⁰ and experimentally demonstrated,¹¹ allowing an array of new applications in quantum information processing.

Two-photon emission (TPE) is a nonlinear process with unique quantum properties, important in different realms of science. TPE from a semiconductor results from electron–hole recombination with the simultaneous emission of two photons. Semiconductor TPE was recently observed¹² and theoretically analyzed,¹³ and current-induced two-photon transparency was demonstrated,¹⁴ paving the way for the realization of room-temperature miniature devices, including semiconductor two-photon lasers¹⁵ and photon pair sources.¹⁶ However, TPE is an inherently weak second-order process, and therefore enhancing mechanisms could significantly widen the range of its applications. Since the

emission spectrum of spontaneous TPE is very wide band due to the large energy uncertainty of the virtual state, regular dielectric optical cavities with a very high quality-factor, Q , and thus very narrow bandwidth¹⁷ may enhance emission at specific wavelengths;¹⁸ however, they are unable to enhance the broad spectrum of TPE. Plasmonic cavities, on the other hand, enhancing the field by significantly reducing the mode volume at low Q ,¹⁹ are optimal.

Here we report the first experimental observation of plasmon-enhanced spontaneous TPE from semiconductors, by coupling the emission to bow-tie nanoantenna arrays, having efficient radiative coupling of plasmons to far-field light.²⁰ The broad band TPE from AlGaAs is significantly reshaped for emission from a region located in the near-field of the nanoantennas if the resonance of the nanostructure is near the center of the TPE spectrum—about half the band gap energy. The enhancement was verified to decrease with spectral detuning of the antenna resonance from the TPE center, in accordance with our theoretical prediction. In order to confine most of the charge carriers to the near-field of the nanoantennas, a relatively thin AlGaAs layer was grown on GaAs substrate, separated by a higher band gap AlGaAs composition, thereby generating a potential well (Figure 1 inset). The near-infrared (NIR) broad emission (Figure 2a) was verified to be TPE by singly stimulated emission experiments¹² (Figure 2b). The presented scheme can be further integrated to yield electrically pumped plasmon enhanced TPE by employing lateral injection techniques, similar to those used in oxide aperture vertical-cavity surface-emitting lasers.²¹

TPE spectrum from a semiconductor is calculated by a second-order term in the time-dependent perturbation theory¹³

* To whom correspondence should be addressed. nevet@tx.technion.ac.il.

Received for review: 02/17/2010

Published on Web: 04/16/2010

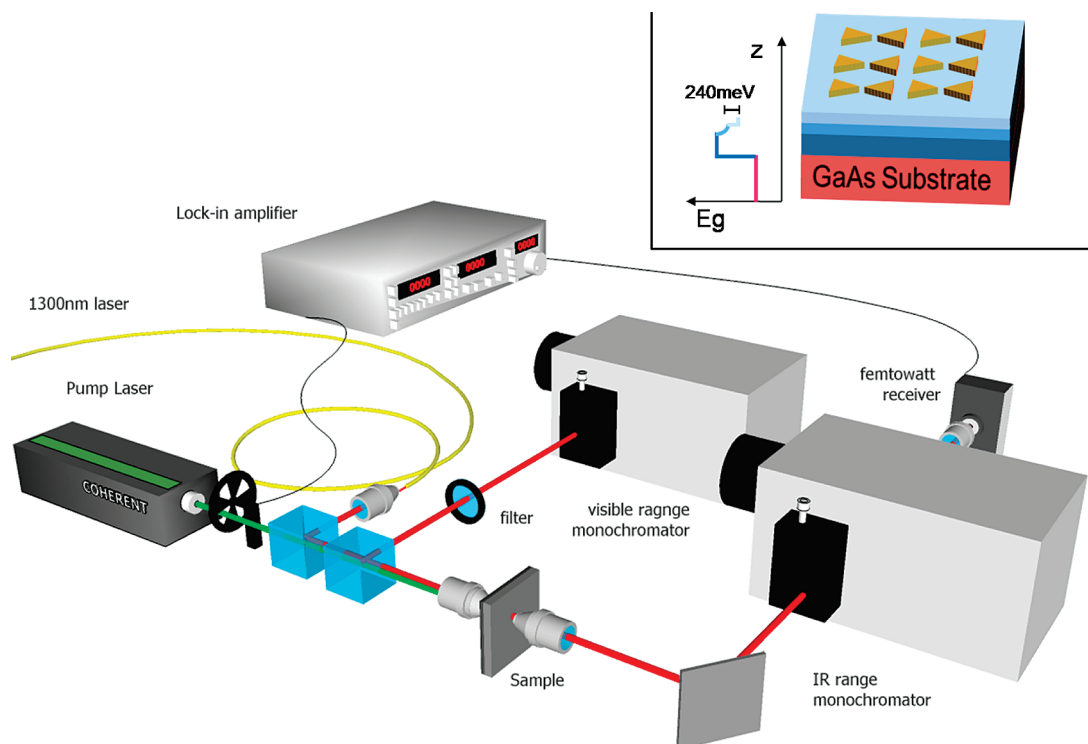


FIGURE 1. Schematics of the measurement setup. The inset is a schematic drawing of the sample structure and the layer band gap in the growth direction.

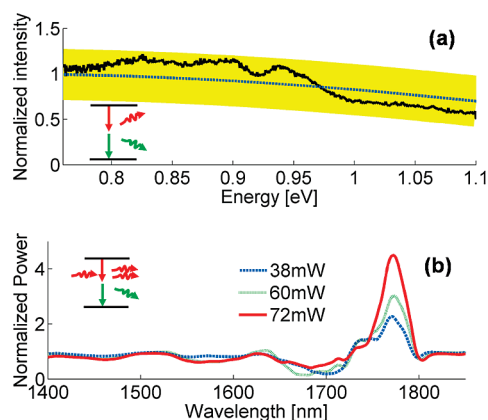


FIGURE 2. (a) Spectrum of the spontaneous TPE from a bare sample. The solid black line is the measured spectrum, the dashed blue line is the calculated spectrum with its variance shown by the shaded yellow area. The inset is a diagram of spontaneous TPE. (b) Measurement spectrum of TPE singly stimulated by 1.31 mm laser at various power levels. The inset is a diagram of singly stimulated TPE.

$$R(\omega_1) = \frac{2\pi}{\hbar^2} D(\omega_1) D(\omega_0 - \omega_1) \sum_{\text{carrier states}} |M|^2 \quad (1)$$

where $\hbar\omega_0$ is the energy of the one-photon transition, $D(\omega)$ the density of radiation modes, and the summation over carrier states takes into account the electron density of states and the Fermi–Dirac distributions. M , the matrix element for the transition, is given by

$$M = \frac{e^2}{2m_0c^2} \left(\frac{2\pi\hbar c^2}{V} \right) \frac{1}{\sqrt{\omega_1(\omega_0 - \omega_1)}} M' \quad (2)$$

where e is the electron charge, m_0 the free electron mass, V the field quantization volume, and M' the dimensionless matrix element for the second-order process

$$M' = \frac{2}{m_0 \sqrt{n(\omega_1)n(\omega_0 - \omega_1)n_g(\omega_1)n_g(\omega_0 - \omega_1)}} \sum_n \left(\frac{\langle f | \hat{p} \cdot \vec{\epsilon}_2 e^{-ik_2x} | n \rangle \langle n | \hat{p} \cdot \vec{\epsilon}_1 e^{-ik_1x} | i \rangle}{E_i - E_n - \hbar\omega_1 + i\Gamma} + \frac{\langle f | \hat{p} \cdot \vec{\epsilon}_2 e^{-ik_2x} | n \rangle \langle n | \hat{p} \cdot \vec{\epsilon}_1 e^{-ik_1x} | i \rangle}{E_i - E_n - \hbar(\omega_0 - \omega_1) + i\Gamma} \right) \quad (3)$$

where \hat{p} is the momentum operator, $\vec{\epsilon}$ the photon field, Γ the charge-carrier dephasing rate,¹² and E_m the energy of the electron state m , with m being one of i , n , and f , standing for initial, intermediate, and final states, respectively.

In a bulk semiconductor with refractive index $n(\omega)$ and group index $n_g(\omega)$, the density of photonic states is given by

$$D_{\text{bulk}}(\omega) = \frac{\omega^2 n^2(\omega) n_g(\omega)}{\pi^2 c^3} V \quad (4)$$

where c is the vacuum velocity of light, whereas in a plasmonic cavity, a Lorentzian normalized density of states is a good approximation²²

$$D_{\text{cavity}}(\omega) = \frac{1}{\pi} \frac{\omega_R/2Q}{(\omega - \omega_R)^2 + (\omega_R/2Q)^2} \quad (5)$$

where ω_R is the resonance angular frequency of the plasmonic cavity. The spectral dependence of the plasmonic cavity enhancement relative to the bulk is therefore

$$\frac{R_{\text{cavity}}(\omega_1)}{R_{\text{bulk}}(\omega_1)} = \frac{F_p(\omega_1) F_p(\omega_0 - \omega_1) D_{\text{cavity}}(\omega_1) D_{\text{cavity}}(\omega_0 - \omega_1)}{\omega_1^2 (\omega_0 - \omega_1)^2} \quad (6)$$

where

$$F_p(\omega_1) = \frac{\pi^2 c^3}{n^2(\omega_1) n_g(\omega_1) V_{\text{cavity}}^*(\omega_1)}$$

and

$$1/V_{\text{cavity}}^*(\omega_1) = \frac{1}{\sqrt{V_{\text{cavity}}(\omega_1) V_{\text{cavity}}(\omega_0 - \omega_1)}}$$

For a single-resonance plasmonic cavity, maximal enhancement is achieved for a cavity resonance at the center of the TPE spectrum, $\omega_R = \omega_0/2$, for which the two emitted photons are degenerate in frequency $\omega_1 = \omega_0 - \omega_1 = \omega_R$. It should be noted that the rate involves the multiplication of two spectral functions symmetrically located around the TPE center—thus the TPE enhancement is symmetrical around the central wavelength as well, in contrast to the enhancement of one-photon emission (OPE) which is maximal near the plasmonic resonance wavelength. Moreover, since all dispersive parameters in F_p are multiplied by their complementary value around the center of the TPE spectrum, the moderate spectral dependence of F_p in our scheme is averaged and becomes negligible, and the large spectral width of the enhancement is thus maintained.

In our experiments, the structure was comprised of a 200 nm thick $\text{Al}_{0.11}\text{Ga}_{0.89}\text{As}$ active layer, with one photon photoluminescence centered at ~ 826 nm (1.5 eV), and TPE centered at ~ 1653 nm (0.75 eV). The layer was epitaxially grown on a 300 nm graded index layer $\text{Al}_{0.5}\text{Ga}_{0.7}\text{As}$ – $\text{Al}_{0.6}\text{Ga}_{0.4}\text{As}$ followed by 1.5 μm $\text{Al}_{0.6}\text{Ga}_{0.4}\text{As}$, on a GaAs substrate, generating a potential well for carriers in the active layer (Figure 1 inset). The 60 nm high gold nanoantenna

arrays with an overall dimension of 50 $\mu\text{m} \times 50 \mu\text{m}$ were fabricated on the surface of the active layer (Figure 3a,b) using e-beam lithography. The sample was optically pumped by a 100 mW frequency-doubled Nd:YAG laser (532 nm), chopped at 375 Hz, and focused onto the sample with a spot diameter of $\sim 5 \mu\text{m}$.

First, spontaneous emission from a bare sample was collected through the substrate in a transmission configuration (Figure 1), absorbing OPE completely, and detected through a spectrometer using a femtowatt NIR receiver, in a lock-in detection scheme (Figure 2a). To verify that this emission is indeed TPE, we conducted singly stimulated experiments where a 1.3 μm (~ 0.95 eV) continuous-wave laser was added to the pumping path, and the complementary emission around 1.77 μm (~ 0.7 eV) was detected in agreement with theory (Figure 2b).

The plasmonic resonance of the bow-tie antenna, resulting from both longitudinal and transversal modes (Figure 3c,d), was designed to be located near the center of the TPE spectrum (Figure 4a), for maximal enhancement. Transmission measurements using white light showed an absorption resonance located at 1620 nm with a Q factor of ~ 5 , similar to our finite-difference time-domain (FDTD) simulation results. Following this characterization, the 532 nm pump was focused onto an area within the bow-tie array and the TPE was collected through the GaAs substrate, absorbing the OPE, and the measurement was normalized by a reference spectrum collected from a bare part of the sample. The result demonstrates a clear reshaping of the spectrum (Figure 4b) in respect to the spectrum from a bare sample (Figure 2a) and exhibits a clear maximum near twice the OPE central wavelength (Figure 4b inset) an enhancement by a factor of ~ 20 relative to the plateau of the spectrum far from the resonance, in good agreement with the theory (eq 6). Considering the FDTD-calculated effective-volume²³ $V_{\text{cavity}} \sim 10^{-3} \mu\text{m}^3$, and the effective fill factor, the total emission from regions unaffected by plasmonic enhancement (background) was calculated to be ~ 30 times larger than the total emission from regions enhanced by the plasmonic array (signal). Given this background emission, the measurement corresponds to maximal enhancement by nearly 3 orders of magnitude for carrier emission coupled to the antennas. This effect cannot be attributed to antenna enhancement of the pump coupling, which cannot result in reshaping of the emission spectrum. Moreover, the OPE which should be linearly related to the coupled pump power was slightly reduced. To further verify that the observed enhancement results from second-order transitions, we designed and fabricated additional nanoantenna arrays with different resonance wavelengths^{24,25} for which the detuning of the resonance resulted in a weaker enhancement, however still located around the center of the TPE.

For narrow-band one-photon emitters, the overall emission can be enhanced as was calculated and demonstrated in various experiments according to the Purcell effect theory.

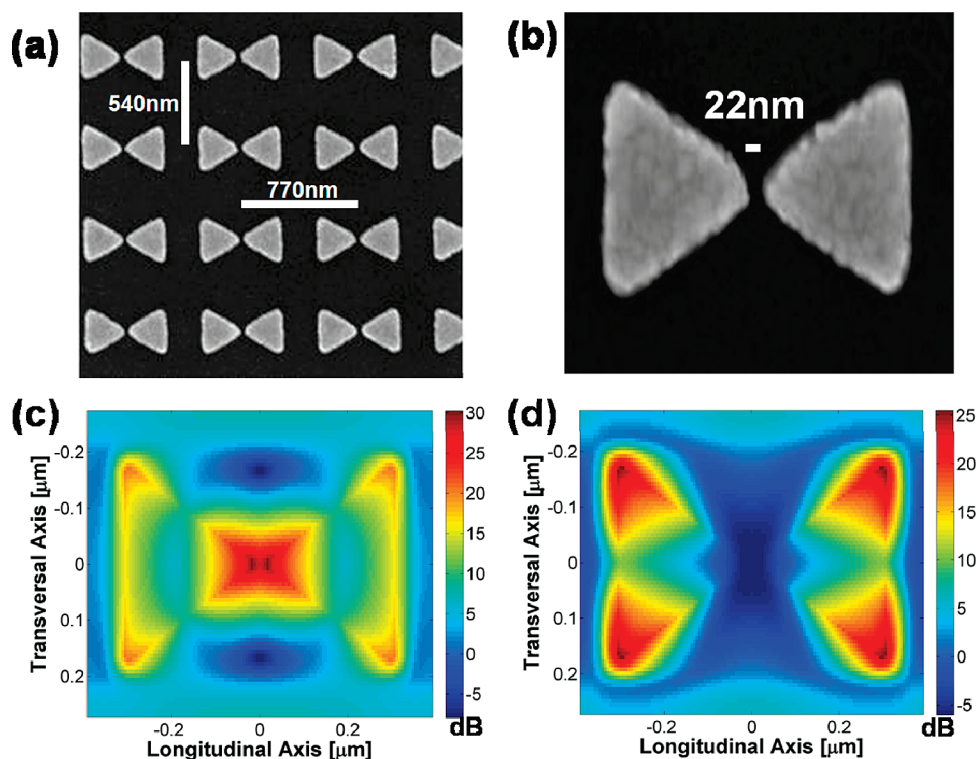


FIGURE 3. (a, b) SEM image of the particles at two different magnifications. (c) Electric field intensity at resonance at a plane located 10 nm below the antenna calculated using FDTD simulations for longitudinal mode. (d) Electric field intensity at resonance at a plane located 10 nm below the antenna calculated using FDTD simulations for transversal mode. The image is presented in logarithmic scale relative to the excitation field.

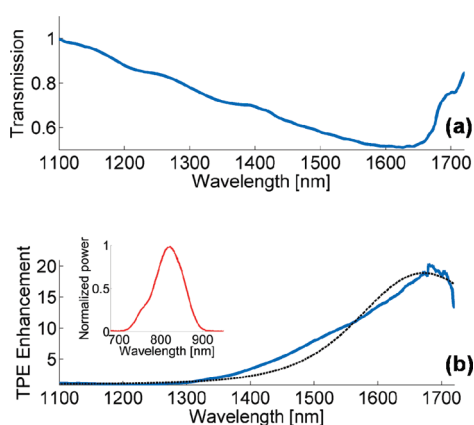


FIGURE 4. (a) Transmission spectrum of the passive bow-tie particle array. (b) Spectrum of the enhancement in TPE by the bow-tie array: measurement, solid blue line; FDTD calculation, dashed black line. The inset is the one-photon emission spectrum.

However, for extremely wide band emission, and if the entire spectrum is taken into consideration, the overall linear one-photon emission is limited by the sum rules,^{26,27} which are no longer applicable in the nonlinear TPE case. Our results show that the nonlinear nature of TPE allows the enhancement of the entire ultra-wide-band spectrum. Although the total number of photonic modes cannot be changed, only spectrally reshaped, the fact that the overall TPE rate is proportional to the integration of the multiplica-

tion of two state density distributions symmetrically located around the center allows this reshaping to lead to net enhancement of the wide band TPE.

In conclusion, we have observed and characterized the broad-band enhancement of spontaneous two-photon emission from AlGaAs, by coupling to plasmonic nanoantennas, in good agreement with theory. The broad enhancement results from the broad-band response of the cavity resonance at very low mode volumes, and it is insensitive to several dispersive parameters owing to the intermixing of the two complementary photons. The enhancement is shown to be most significant for resonances located around the center of the TPE spectrum and reduced with increased detuning of the resonance.

REFERENCES AND NOTES

- (1) Neogi, A.; Lee, C. W.; Everitt, H. O.; Kuroda, T.; Takemuchi, A.; Yablonovich, E. *Phys. Rev. B* **2002**, *66*, 153305.
- (2) Okamoto, K.; Niki, I.; Scherer, A.; Narukawa, Y.; Mukai, T.; Kawakami, Y. *Appl. Phys. Lett.* **2005**, *87*, No. 071102.
- (3) Pillai, S.; Catchpole, K. R.; Trupke, T.; Zhang, G.; Zhao, J.; Green, M. A. *Appl. Phys. Lett.* **2006**, *88*, 161102.
- (4) Sun, G.; Khurgin, J. B.; Soref, R. A. *J. Opt. Soc. Am. B* **2008**, *25*, 1748–1755.
- (5) Moskovičs, M. *Rev. Mod. Phys.* **1985**, *57*, 783–826.
- (6) Zayats, A. V.; Smolyaninov, I. I.; Maradudin, A. A. *Phys. Rep.* **2005**, *408*, 131–314.
- (7) Kim, S.; Jin, J.; Kim, Y. J.; Park, I. Y.; Kim, Y.; Kim, S. W. *Nature* **2008**, *453*, 757.

- (8) Altwischer, E.; van Exter, M. P.; Woerdman, J. P. *Nature* **2002**, *418*, 304–306.
- (9) Fasel, S.; Robin, F.; Moreno, E.; Erni, D.; Gisin, N.; Zbinden, H. *Phys. Rev. Lett.* **2005**, *94*, 110501.
- (10) Bergman, D. J.; Stockman, M. I. *Phys. Rev. Lett.* **2003**, *90*, 027402.
- (11) Hill, M. T. *Nat. Nanotechnol.* **2009**, *4*, 706–707.
- (12) Hayat, A.; Ginzburg, P.; Orenstein, M. *Nat. Photonics* **2008**, *2*, 238–241.
- (13) Hayat, A.; Ginzburg, P.; Orenstein, M. *Phys. Rev. Lett.* **2009**, *103*, 023601.
- (14) Hayat, A.; Nevet, A.; Orenstein, M. *Phys. Rev. Lett.* **2009**, *102*, 183002.
- (15) Gauthier, D. J.; Wu, Q.; Morin, S. E.; Mossberg, T. W. *Phys. Rev. Lett.* **1992**, *68*, 464.
- (16) van Driel, H. M. *Nat. Photonics* **2008**, *2*, 212.
- (17) Kippenberg, T. J.; Spillane, S. M.; Vahala, K. J. *Appl. Phys. Lett.* **2004**, *85*, 6113.
- (18) Lin, Z.; Vučković, J. *Phys. Rev. B* **2010**, *81*, 035301.
- (19) Feigenbaum, E.; Orenstein, M. *Phys. Rev. Lett.* **2008**, *101*, 163902.
- (20) Muskens, O. L.; Giannini, V.; Sánchez-Gil, J. A.; Gómez Rivas, J. *Nano Lett.* **2007**, *7*, 2871–2875.
- (21) MacDougal, M. H.; Geske, J.; Lin, C.-K.; Bond, A. E.; Dapkus, P. D. *IEEE Photonics Technol. Lett.* **1998**, *10*, 9.
- (22) Gong, Y.; Lu, J.; Cheng, S.; Nishi, Y.; Vučković, J. *Appl. Phys. Lett.* **2009**, *94*, 013106.
- (23) Maier, S. A. *Opt. Express* **2006**, *14*, 1957–1964.
- (24) Khlebtsov, B. N.; Khlebtsov, N. G. *J. Phys. Chem. C* **2007**, *111*, 11516.
- (25) Xia, Y.; Halas, N. *MRS Bull.* **2005**, *30*, 338.
- (26) Barnett, S. M.; Loudon, R. *Phys. Rev. Lett.* **1996**, *77*, 2444–2446.
- (27) Scheel, S. *Phys. Rev. A* **2008**, *78*, 013841.